

NON-DESTRUCTIVE AIR-PERMEABILITY MEASUREMENT: FROM GAS-FLOW MODELLING TO IMPROVED TESTING

R. Torrent (1)

(1) Materials Advanced Services Ltd., Buenos Aires, Argentina

Abstract

The fundamentals of a test method to measure, non-destructively, the coefficient of air-permeability of the 'covercrete' were established in the 90's leading to the development of a commercial instrument, the "Torrent Permeability Tester" (TPT).

The model and formula used today to calculate the coefficient of air-permeability kT were developed in 1995. They are based on assuming a unidirectional flow through a material regarded as homogeneous. Under such conditions, the response of the test (pressure increase) with the square root of time should be linear.

Deviations from the theoretical response were found for low-permeability concretes not completely dry, and attributed to an artificial increase in pressure caused by the evaporation of moisture, present in the concrete pores, into the test chamber.

A new instrument, "*PermeaTORR*" (*PT*), has been designed and built to ensure a better fulfilment of the theoretical conditions assumed in the model, in order to get more reliable and accurate results.

The incorporated improvements led to an accentuated linearity of the test, enabling to shorten the test from 12 to 6 minutes.

The paper discusses the fundamentals of the model used to calculate kT , the different response of the two instruments (TPT and *PT*) and the correlation between them.

An example of non-linear behaviour, obtained with *PT* for a concrete cast against "Zemdrain" is presented.

1. INTRODUCTION

Since the early 90's, the Swiss Federal Highway Administration has been supporting R&D projects oriented at developing a suitable approach for specifying and controlling the quality of the cover concrete on site, [1-6]. This work, complemented by other investigations, led to the standardization in 2003 of a non-destructive test method, originally developed by Torrent [7], to measure the air-permeability of the cover concrete on site [8].

In the same year, a new Swiss Code for Concrete Construction, based on Eurocode 2, was issued [9]. This Code describes the measures to be adopted in order to ensure durability and, acknowledging the importance of the "impermeability" of the cover concrete, specifically states that "the impermeability of the cover concrete shall be checked, by means of

permeability tests (e.g. air permeability measurements), on the structure or on cores taken from the structure”.

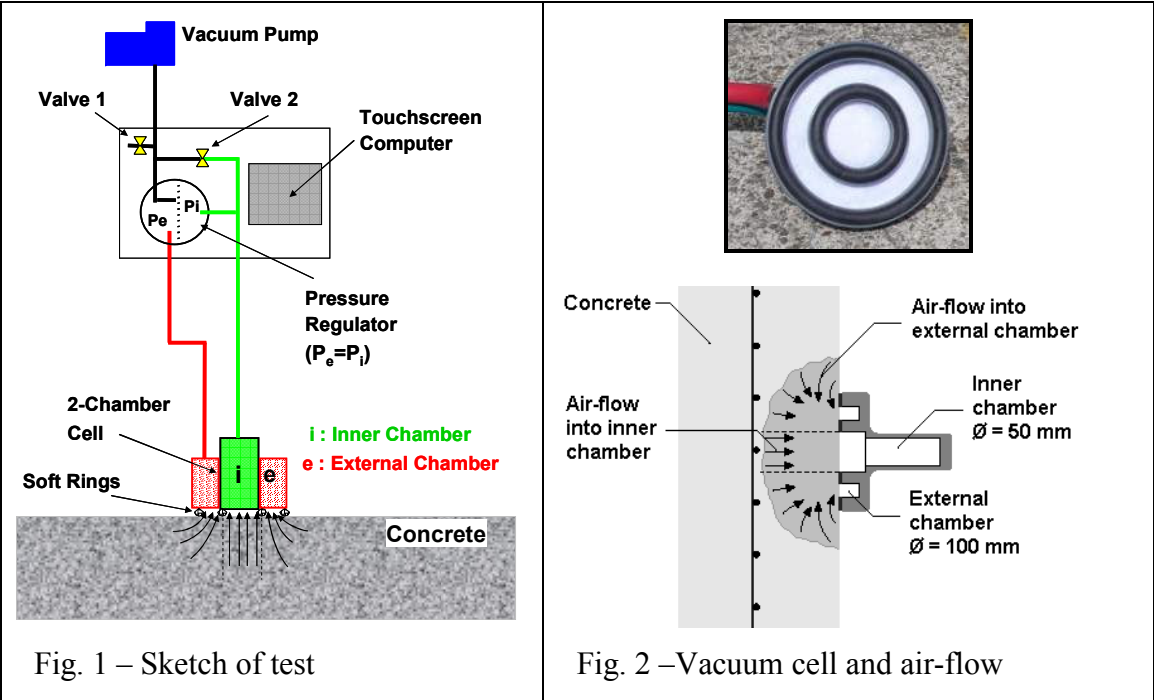
2. DESCRIPTION OF THE TEST METHOD

The method serves to measure the coefficient of air-permeability of the cover concrete on site, in a non-destructive manner and operates as follows.

Vacuum is created inside the 2-chamber vacuum cell (Fig. 1), which is sealed onto the concrete surface by means of a pair of concentric soft rings, creating two separate chambers. At a time between 35 and 60 sec (with a vacuum of ca. 5 - 50 mbar, depending on the concrete, instrument, etc.) valve 2 is closed and the pneumatic system of the inner chamber is isolated from the pump. The air in the pores of the material flows through the cover concrete into the inner chamber, raising its pressure P_i . The rate of pressure rise ΔP_i (measurement starts at $t_0 = 60$ s) is directly linked to the coefficient of air-permeability of the cover concrete.

A pressure regulator maintains the pressure of the external chamber permanently balanced with that of the inner chamber ($P_e = P_i$). Thus, a controlled unidirectional flow into the inner chamber is ensured (Fig. 2) and the coefficient of permeability to air kT (m^2) can be calculated as described below.

Two commercial instruments have been launched on the market: in 1995 the “Torrent Permeability Tester” (TPT) by Proceq S.A. and in 2009 the “PermeATORR” (PT) by Materials Advanced Services Ltd.



3. MODEL TO CALCULATE kT

To calculate the coefficient of air-permeability kT , some assumptions (particularly the last two simplifying the real situation) are made in modelling the air-flow into the vacuum cell:

- The concrete affected by the test is homogeneous (in particular its porosity and permeability) and, at the beginning of the test ($t=0$), all its free pores air at the atmospheric pressure P_a
- The thickness of the tested element is \geq than the maximum penetration of the test L
- The distribution of pressure along the air path of the test Y is linear (strictly valid for steady-state conditions and laminar flow)
- The external chamber “e” (see Figs. 1 and 2) is always at the same pressure as the inner measurement chamber, and the flow of air into the latter is laminar and perpendicular to the concrete surface along the whole duration of the test (see Fig. 3b)

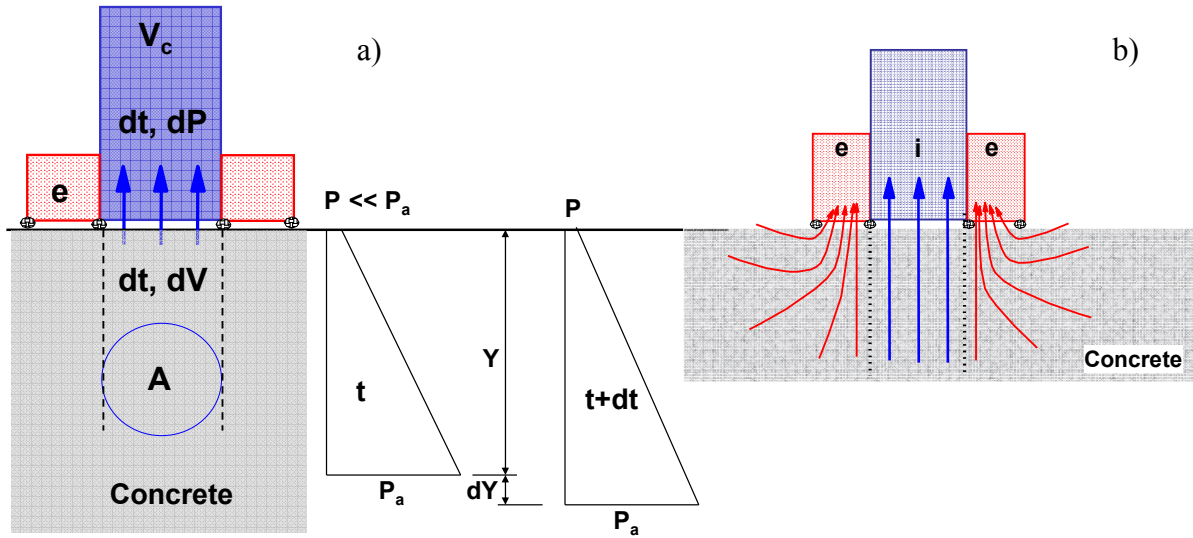


Fig. 3 – Main elements of the Model (a) and schematic air flow assumed (b)

Fig. 3a shows the main elements of the model. At time t , the P_a front has reached a depth Y ; an instant dt later, the depth has grown dY , so as to contribute the volume of air dV that has entered the inner chamber in that time interval. The instrument registers an increase in pressure in the inner chamber of dP , due to the ingress of dV . At all times the pressure P in the inner chamber remains negligible (10 to 60 mbar) compared to P_a .

Applying the Hagen-Poiseuille law for compressible fluids, under the assumptions of the model, the coefficient of air-permeability is calculated with Equation 1; a full derivation can be found in [2, 10].

$$kT = \left(\frac{V_c}{A} \right)^2 \frac{\mu}{2 \varepsilon P_a} \left(\frac{\ln \frac{P_a + \Delta P_i}{P_a - \Delta P_i}}{\sqrt{t_f} - \sqrt{t_0}} \right)^2 \quad (1)$$

where:

kT : coefficient of air-permeability (m^2)

V_c : volume of inner cell system (m^3)

A : cross-sectional area of inner cell (m^2)

μ : viscosity of air ($= 2.0 \cdot 10^{-5} \text{ Ns/m}^2$)

ε : estimated porosity of the cover concrete (assumed = 0.15)

P_a : atmospheric pressure (N/m²)

ΔP_i : pressure rise in the inner cell at the end of the test (N/m²)

t_f : time (s) at the end of the test (2 to 6 or 12 min, depending on the instrument brand)

t_o : time (s) at the beginning of the test (= 60 s)

The maximum penetration depth L (mm) of the P_a front is calculated with Equation 2.

$$L = 1000 \left[\frac{2 \cdot kT \cdot P_a \cdot t_f}{\varepsilon \cdot \mu} \right]^{1/2} \quad (2)$$

It is interesting to notice that Eq. 2 is identical to that originally proposed to calculate the coefficient of permeability of concrete, from the water penetration depth, under the “Water penetration under pressure” test (EN 12390-8) [11, 12].

By developing the logarithm in series, Eq. 1 can be transformed into Eq. 3, [13].

$$\Delta P_i(t) = P_a^{3/2} \cdot (A / V_c) \cdot (kT \cdot \varepsilon / 2 \mu)^{1/2} \cdot (\sqrt{t} - \sqrt{t_o}) \quad (3)$$

Eq. 3 means that, if the model is correct, and ε and kT are constant, a plot of the pressure rise in the inner chamber $\Delta P_i(t)$ as function of $(\sqrt{t} - \sqrt{t_o})$ should be linear; t is the time of test (s).

4. APPARENT NON-LINEAR RESPONSE OF THE INSTRUMENT

Romer [14], applying the TPT instrument, found that low-permeability concretes containing moisture in their fine pore structure, showed a typical non-linear behaviour in their $\Delta P_i - \sqrt{t}$ relation. He attributed this behaviour to the evaporation of water into the evacuated cell, which was working below the water vapour pressure. He identified an initial steep increase in pressure, attributable to the evaporation of water inside the chamber, followed by a lower rate of pressure increase, due to the true flow of air into the chamber. The application of Eq. 1 would be giving an overestimate of the coefficient of air-permeability of such concretes.

In order to avoid that perturbation, the new instrument *PT*, taking advantage of its fully automatic process control, was designed to operate above the water vapour pressure. This has resulted in a typical better linearity of the response, as shown in Fig. 6.

Fig. 4 shows the plot of the $\Delta P_i - \sqrt{t}$ relations obtained in the laboratory with the TPT and *PT* on a cast concrete slab ($w/c = 0.45$). Fig. 4a corresponds to the bottom face of the slab as cast, whilst Fig. 4b corresponds to the upper, trowelled face. The charts show the following data: P_o (pressure in the inner chamber at 60 s), kT (value reported by the instruments) and, at the extreme right of the curves, a value of kT calculated from the slope¹ of the ΔP_i values recorded between 360 and 720 of test.

Fig. 4a shows that the plot recorded by the TPT presents a pronounced curvature leading to a kT value of $0.028 \cdot 10^{-16} \text{ m}^2$; notice that the initial pressure is 10.8 mbar, i.e. well below the water vapor pressure. The plot recorded by the *PT* presents a less marked curvature, leading to a lower kT value of $0.0071 \cdot 10^{-16} \text{ m}^2$; the initial pressure is 31.2 mbar; i.e. slightly above the

¹ Both instruments have different constant A/V_c , so equal slope does not mean equal kT (see Eq. 3)

water vapor pressure. It is interesting to see that the slopes at the end of the test show similar and quite lower values: 0.0032 and $0.0016 \cdot 10^{-16} \text{ m}^2$ for the TPT and *PT*, respectively.

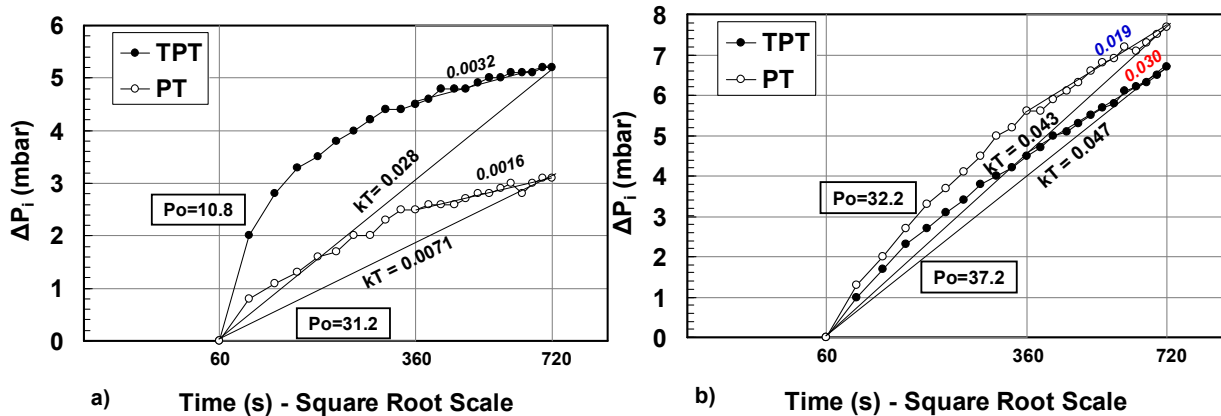


Fig. 4 - $\Delta P_i - \sqrt{t}$ relations obtained with TPT and *PT* on two faces of a sample.

Fig. 4b shows the same data, but obtained on the upper side of the slab. Due to different compaction and curing, the upper side is usually of higher permeability than the bottom side; moreover, the finishing left a not too smooth surface. Under these circumstances, the initial pressure $P_o = 37.2$ mbar reached by the TPT was naturally higher than that on the bottom side (10.8 mbar). The *PT*, on the other hand, due to its automatic regulation, showed very similar values of P_o : 31.2 and 32.2 mbar for the bottom and upper side of the slab, respectively. Both instruments yielded very similar results of kT of the upper face: $0.043 \cdot 10^{-16} \text{ m}^2$ for the TPT and $0.047 \cdot 10^{-16} \text{ m}^2$ for the *PT*. These results support Romer’s explanation for the strong non-linearity of the TPT response, attributed to operating with P_i values below the vapor pressure.

The consequence of this difference in response of both instruments is that the TPT tends to overestimate the coefficient of air-permeability for low-permeability concretes, compared with the results yielded by the *PT*, as shown in Fig. 5.

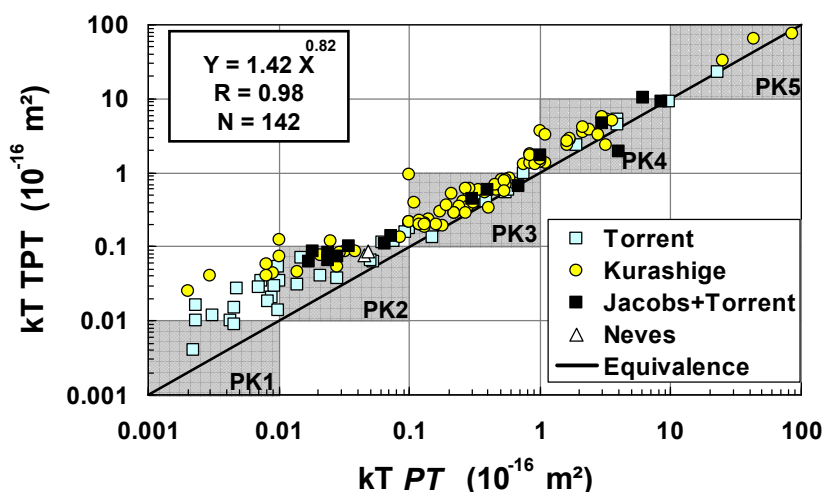


Fig. 5 – Correlation between the kT values obtained with the TPT and *PT* instruments by different researchers

The results displayed in Fig. 5 come from different sources, applying different TPT and *PT* instruments on the same spots of samples [15, 16]. Worth mentioning are the results recorded

by Jacobs and Torrent, also included in the chart, obtained on site on different segments of a tunnel’s vertical liner [6].

5. ADVANTAGES OF LINEAR RESPONSE

As clearly shown in Fig. 4, deviation from linearity makes the calculation of kT dependent on the time interval chosen (slope of the line connecting the first and last point involved).

The close linearity of the $\Delta P_i - \sqrt{t}$ plot, recorded in the large majority of tests performed with the *PT* has prompted its designers to display the chart on its computer screen with reference lines representing different kT values (see Fig. 6). This has two advantages:

- The user can visually control linearity and guess the approximate value of kT shortly after starting the test
- If the plot is close to linear, the user can stop the test after 6 minutes instead of waiting 12 minutes, getting a very similar kT value (and halving the test duration)

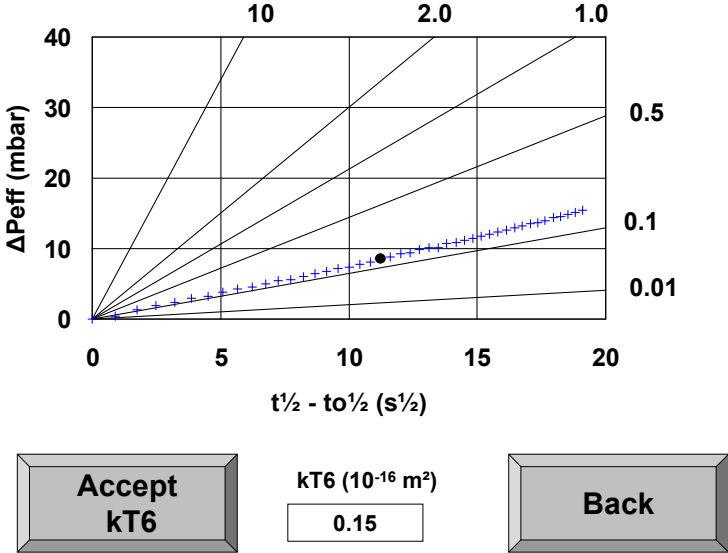


Fig. 6 – Display of *PT* instrument, with test results (+) and reference kT lines. The black dot is the value at $t=360$ s ($kT6 = 0.15 \cdot 10^{-16} \text{ m}^2$), which may be accepted by the user.

6. NON-LINEARITY AS INDICATION OF HETEROGENEITY

A non linear display is not necessarily an artefact due to water evaporation, but could be an indication that the P_a front is finding layers of concrete of higher (positive curvature) or lower (negative curvature) permeability as it advances deeper into the concrete.

A good example of this situation has been found when testing a concrete panel, one of whose faces was cast against a Controlled Permeable Formliner (“Zemdrain”)², to dewater the surface layers whilst the opposite face was cast against the natural formwork. Since the panel had been stored for 16 years in a dry room (20°C, 50% RH) the effect of moisture on the measurements could be ruled out.

² The membrane allows water and air, pushed by vibration and hydraulic pressure, to be removed from the concrete surface whilst retaining the cement particles, thus lowering the w/c ratio of the surface layers [17].

Fig. 7 shows $\Delta P_i - (\sqrt{t} - \sqrt{t_0})$ plots, recorded with the *PT* instrument. The three curves correspond to the tests that showed the lowest, highest and near-average values of *kT*. The white dots correspond to tests conducted on the natural surface in contact with the formwork; the black dots to those conducted on the face in contact with Zemdrain. The geometric mean values of *kT* were $6.0 \cdot 10^{-16} \text{ m}^2$ and $0.79 \cdot 10^{-16} \text{ m}^2$, for the Natural and Zemdrain faces, respectively.

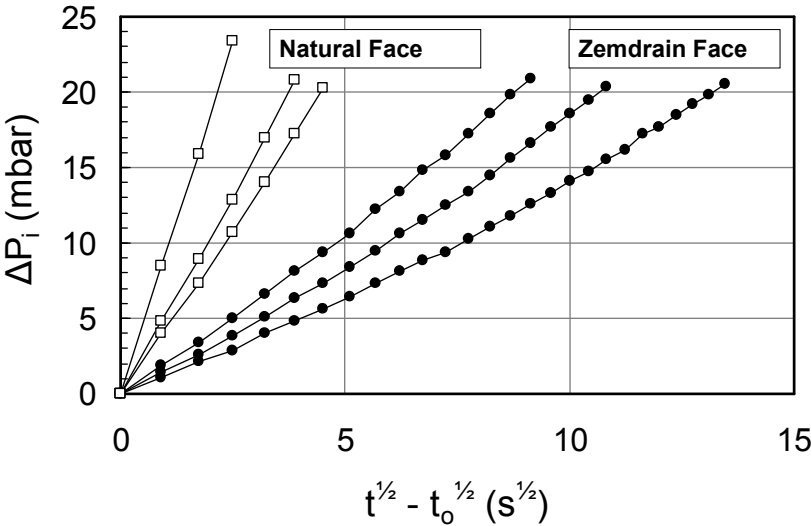


Fig. 7 - $\Delta P_i - (\sqrt{t} - \sqrt{t_0})$ plot recorded on a panel one of whose faces was cast against a Zemdrain membrane.

The plots of the Zemdrain face tests show a slight but noticeable positive curvature, contrary to the plots of the Natural face tests that are more linear. This might indicate that the *kT* of the Zemdrain face tends to increase with depth, which is consistent with the action of the membrane (carbonation may also have an influence on both surfaces). Nevertheless, the final slope of the Zemdrain plots is lower than that recorded on the Natural face, which could be interpreted as that the effect of Zemdrain extends relatively deep (about 50 mm, which is an average value of the test penetration *L*) inside the concrete, as confirmed in [18].

7. CONCLUSIONS

Based on air-flow modeling, several improvements in the SIA 262/1-E method have been included in the *PT* instrument, increasing its reliability, practicality and productivity, as follows:

- The continuous monitoring of the pressure in both chambers of the vacuum cell checks the fulfillment of the fundamental condition that $P_e = P_i$, which is at the heart of the test method. This ensures a controlled, unidirectional flow of air into the inner chamber
- The automatic operation of the instrument guarantees that the P_i is above the water vapor pressure during the measurements, thus increasing the linearity of the instrument response
- The linearity of the $\Delta P_i - (\sqrt{t} - \sqrt{t_0})$ plot, obtained in the large majority of cases, is an indication that the model applied to derive Eq. 1 has a reasonably sound theoretical basis

- The display of the progress of the test as $\Delta P_i - (\sqrt{t} - \sqrt{t_0})$ plot with reference lines, allows guessing the approximate kT value early during the test and, in case of linearity, to stop the test at 360 s, thus halving the maximum duration of the test
- Deviations from a linear plot provides useful indication on changes of kT with the depth of concrete affected by the test

Despite their differences in operation, a very good correlation was found between the results of both instruments, with the TPT providing higher kT values than the PT for low permeability concretes, say below $0.5 \cdot 10^{-16} \text{ m}^2$.

REFERENCES

- [1] Torrent, R. u. Ebensperger, L., "Studie über Methoden zur Messung und Beurteilung der Kennwerte des Überdeckungsbetons auf der Baustelle", Office Fédéral des Routes, VSS Rapport 506, Bern, Suisse, 1993.
- [2] Torrent, R. und Frenzer, G., "Methoden zur Messung und Beurteilung der Kennwerte des Ueberdeckungsbetons auf der Baustelle -Teil II", Office Fédéral des Routes, VSS Rapport 516, Bern, Suisse, 1995.
- [3] Brühwiler, E., Denarié, E., Wälchli, Th., Maître, M. et Conciatori, D., "Dauerhafte Kunstbauten bei geringem Unterhalt - Ausgewählte Kapitel", Office Fédéral des Routes, VSS Report 587, Bern, Suisse, 2005, Chapter 1, pp. 1-48,.
- [4] Denarié E., Maître M., Conciatori D., Brühwiler E., "Air permeability measurements for the assessment of the in situ permeability of cover concrete", in Proc. Intern. Conf. Concrete Repair, Rehabilitation and Retrofitting – ICCRRR 2005, 21-23 Nov. 2005, Cape Town, South Africa.
- [5] Jacobs, F., "Luftpermeabilität als Kenngrösse für die Qualität des Überdeckungsbetons von Betonbauwerken", Office Fédéral des Routes, VSS Rapport 604, Bern, Suisse, 2006.
- [6] Jacobs, F., Denarié, E., Leemann, A. und Teruzzi T., "Empfehlungen zur Qualitätskontrolle von Beton mit Luftpermeabilitätsmessungen", Office Fédéral des Routes, VSS Report 641, Bern, Suisse, 2009.
- [7] Torrent, R.J., "A two-chamber vacuum cell for measuring the coefficient of permeability to air of the concrete cover on site", *Materials and Structures*, **25** (7) (1992) 358-365.,
- [8] Norme Suisse SIA 262/1(2003): "Construction en béton – Spécifications complémentaires", Annexe E: 'Perméabilité à l'air dans les Structures', pp. 30-31.
- [9] Norme Suisse SIA 262 (2003): "Construction en béton".
- [10] Torrent, R., "PermeaTORR: Modelling of Air-Flow and derivation of formulae", M-A-S Report, July 2009, 9 p., <http://www.m-a-s.com.ar/pdf/Derivation%20of%20Formulae.pdf>
- [11] Valenta, O., "The permeability of concrete in aggressive conditions", in 'Large Dams', Proceedings of 10th International Congress, Montreal, 1970, 103-117.
- [12] J. P. Castro-Gomes, L. A. Pereira de Oliveira and C. N. Gonilho-Pereira, "Discussion of Aggregate and Concrete Water Absorption and Permeability Testing Methodology", Housing Construction – An Interdisciplinary Task, Coimbra, Portugal, September 9-13, 2002.
- [13] Torrent, R., "Justification of the Reduction of kT Test's Maximum Duration", M-A-S Report, Sept. 2010, 7 p., <http://www.m-a-s.com.ar/pdf/Justification%20of%20kT6.pdf>
- [14] Romer, M., "Effect of moisture and concrete composition on the Torrent permeability measurement", *Materials and Structures*, **38**, (2005) 541-547.
- [15] Kurashige, I., Central Res. Inst. of Electric Power Ind., Japan, Personal Communication.
- [16] Neves, R., EST Barreiro, Inst. Politécnico de Setúbal, Portugal, Personal Communication.
- [17] http://www2.dupont.com/Zemdrain/en_US/products/zemdrain_concept/zemdrain_concept.html
- [18] Griesser, A., Moro, F., Jacobs, F. and Torrent, R. (manuscript submitted to ICCRRR 2012)